2013

Siggma: A Survey Of Ionized Gas In The Galaxy, Made With The Arecibo Telescope

B. Liu

T. McIntyre

Y. Terzian

R. Minchin

L. Anderson

See next page for additional authors

The Astronomical Journal, 146:80 (7pp), 2013 October doi:10.1088/0004-6256/146/4/80

SIGGMA: A SURVEY OF IONIZED GAS IN THE GALAXY, MADE WITH THE ARECIBO TELESCOPE

B. Liu[1,9,10], T. McIntyre[2], Y. Terzian[3], R. Minchin[4], L. Anderson[5], E. Churchwell[6], M. Lebron[7], and D. Anish Roshi[8]
[1] National Astronomical Observatories, Chinese Academy of Sciences, Beijing 100012, China
[2] University of New Mexico, Albuquerque, NM 87131, USA
[3] Cornell University, Ithaca, NY 14853, USA
[4] Arecibo Observatory, HC03 Box 53995, Arecibo 00612, PR, USA
[5] West Virginia University, Morgantown, WV 26506, USA
[6] University of Wisconsin-Madison, Madison, WI 53706, USA
[7] University of Puerto Rico, P.O. Box 23323, 00931-3323, San Juan, PR, USA
[8] National Radio Astronomy Observatory, Green Bank & Charlottesville, VA 22903, USA
Received 2012 November 30; accepted 2013 July 25; published 2013 August 22

ABSTRACT

A Survey of Ionized Gas in the Galaxy, made with the Arecibo telescope (SIGGMA), uses the Arecibo L-band Feed Array (ALFA) to fully sample the Galactic plane ($30^\circ \leqslant l \leqslant 75^\circ$ and $-2^\circ \leqslant b \leqslant 2^\circ$; $175^\circ \leqslant l \leqslant 207^\circ$ and $-2^\circ \leqslant b \leqslant 1^\circ$) observable with the telescope in radio recombination lines (RRLs). Processed data sets are being produced in the form of data cubes of 2° (along l) $\times$ 4° (along b) $\times$ 151 (number of channels), archived and made public. The 151 channels cover a velocity range of 600 km s^{-1} and the velocity resolution of the survey changes from 4.2 km s^{-1} to 5.1 km s^{-1} from the lowest frequency channel to the highest frequency channel. RRL maps with 3.′4 resolution and a line flux density sensitivity of $\sim$0.5 mJy will enable us to identify new H II regions, measure their electron temperatures, study the physics of photodissociation regions with carbon RRLs, and investigate the origin of the extended low-density medium. Twelve Hnα lines fall within the 300 MHz bandpass of ALFA; they are resampled to a common velocity resolution to improve the signal-to-noise ratio (S/N) by a factor of three or more and preserve the line width. SIGGMA will produce the most sensitive fully sampled RRL survey to date. Here, we discuss the observing and data reduction techniques in detail. A test observation toward the H II region complex S255/S257 has detected Hnα and Cnα lines with S/N $>$ 10.

Key words: Galaxy: structure – H II regions – radio lines: ISM

Online-only material: color figure

1. INTRODUCTION

1.1. Background

Recombination lines are emitted when electrons in ionized gas recombine with atomic nuclei in an excited state and cascade down in energy level, n. The most probable transitions are for $\Delta n = 1$ changes in energy level and are called "α" lines. Transitions with $\Delta n = 2$ are known as "β" lines and so on. For hydrogen, α lines with $n \gtrsim 40$ are in the radio regime ($\lambda \gtrsim 3$ mm) and are termed radio recombination lines (RRLs; see Gordon & Sorochenko 2002 for a full account of the generation of RRLs).

There are three main sources of RRL emission in our Galaxy: H II regions, diffuse ionized gas, and photodissociation regions (PDRs). H II regions are zones of plasma surrounding massive young stars. Astrophysical RRLs were first detected toward the Omega H II region in 1964. These observations were reported by Dravskikh et al. (1966) and Sorochenko & Borodzich (1966) and shortly afterward were followed by high signal-to-noise (S/N) RRL detections toward Orion and M17 (Höglund & Mezger 1965). There have been many subsequent RRL surveys of H II regions (e.g., Reifenstein 1970; Wilson et al. 1970; Wilson 1980; Lockman 1989; Anderson et al. 2011). H II regions are the most intense sources of recombination line emission, although at low frequencies diffuse ionized gas becomes a relatively bright source of RRL emission (see Alves et al. 2010; Lee et al. 2012).

In the Galaxy, the diffuse ionized gas consists of a low-density component (<1 cm^{-3}), referred to as the warm ($T_e \sim$ 3000–8000 K) ionized medium. This component has a scale height of $\sim$1000 pc and is usually studied using optical recombination lines and pulsar dispersion measures (Taylor & Manchester 1977; Reynolds 1990). Observations of low-frequency (<a few GHz) RRLs have established the presence of another diffuse ionized component with a density in the range 1 to 10 cm^{-3} close to the Galactic plane and with a scale height of $\sim$100 pc (Gottesman & Gordon 1970). In the literature, this component is referred to as Galactic Ridge RRL emission by Davies et al. (1972), the extended low-density medium (ELDM) by Mezger (1978), evolved H II regions by Shaver (1976), H II envelopes by Lockman (1976) and Anantharamaiah (1986; e.g., Roshi & Anantharamaiah 2000, 2001; Baddi 2012), the extended low-density warm ionized medium by Petuchowski & Bennett (1993) and Heiles (1994), and the warm ionized medium by Heiles et al. (1996). Following Mezger (1978), in the present paper, this diffuse ionized component is referred to as the ELDM. Recently, extensive higher angular resolution (14.′8) RRL observations of the ELDM were performed by Alves et al. (2012). They found that the distribution of the ELDM is strongly correlated with the location of Galactic H II regions, confirming the observations by Lockman (1976), Hart & Pedlar (1976), and Anantharamaiah (1986). The origin of the ELDM is, however, still unclear, in large part because previous studies used low-resolution observations. One possibility is that it originates from the ionization of low-density regions surrounding giant H II regions, from which photons "leak" (see

[9] Also at the State Key Radio Astronomy Laboratory of China.
[10] Also at the Graduate University of Chinese Academy of Sciences.

Anderson et al. 2011 for a discussion on the W43 region), although this scenario does not fit all observations (Roshi et al. 2012).

In addition to hydrogen lines, carbon RRLs have been detected in several directions in the Galaxy. They are generally observed from interfaces between neutral and fully ionized regions, referred to as PDRs. Photons with wavelengths longer than the Lyman limit can escape the H II region and ionize carbon and other atoms with lower ionization potentials than hydrogen. Carbon RRLs were first detected by Palmer et al. (1967) and have been the focus of many subsequent studies (e.g., Pankonin et al. 1977; Roshi & Kantharia 2011; Wenger et al. 2013).

1.2. Motivation for the Survey

The Survey of Ionized Gas in the Galaxy, made with Arecibo (SIGGMA) will fully sample the entire Galactic plane observable with the 305 m William E. Gordon Telescope at the Arecibo Observatory ($30^\circ \leqslant l \leqslant 75^\circ$ and $-2^\circ \leqslant b \leqslant 2^\circ$ in the inner Galaxy; $175^\circ \leqslant l \leqslant 207^\circ$ and $-2^\circ \leqslant b \leqslant 1^\circ$ in the outer Galaxy) and will be the most sensitive large-scale RRL survey ever made. The survey data will permit a wide range of science, including studies of: (1) H II regions, planetary nebulae, and novae; (2) the Galactic temperature; (3) the large scale structure of the Milky Way; (4) carbon recombination line emitting regions; and, possibly, (5) the ELDM.

RRLs can distinguish between thermal and non-thermal sources. In the section of the inner Galactic plane observable with the Arecibo telescope, there are thousands of continuum sources that were revealed by the *L*-band NRAO VLA Sky Survey (NVSS; Condon et al. 1998). To date, only a few hundred H II regions have been identified in this zone (Lockman 1989; Bania et al. 2010). With a much greater sensitivity than existing surveys, SIGGMA will detect hydrogen RRLs in sources with peak line intensities $\gtrsim$1.5 mJy (3 σ threshold).

H II regions are ideal tracers of spiral arm structure in galaxies. SIGGMA will offer a large-area sample of Galactic H II regions which, together with the ALFA HI survey of the Galactic plane (Peek et al. 2011), will permit a comprehensive study of Galactic structure and kinematics within the Galactic longitude range 30°–75°. This survey will also be useful for checking the current velocity field models of the Galaxy since a rotation curve for the 4.5–8 kpc galactocentric distance range can be derived from the data.

Churchwell & Wamsley (1975) found, for the first time, that the average electron temperatures (T_e) of H II regions gradually increase with galactocentric radius R in the Galaxy. The same trend of T_e was also obtained by Shaver et al. (1983), who directly related this result to the metallicity gradient with R. Using high angular resolution RRL observations toward ultracompact H II (UCHII) regions, Afflerbach et al. (1996) derived the slope of the temperature gradient with R to be 320 K kpc^{-1}. Afflerbach et al. (1997) directly determined the metal abundance in these UCHII regions using IR fine structure line observations. These authors showed, for the first time, that the inferred temperature gradient from the measured metallicity gradient is consistent with that obtained using RRL observations. However, the slope of the electron temperature gradient obtained from data toward UCHII regions is shallower than that determined from data toward classical H II regions (Shaver et al. 1983; Afflerbach et al. 1996). The difference in slope obtained from the two sets of observations needs to be resolved. Moreover, there is still a considerable scatter both in the temperature and metal abundance gradients. This scatter is partly due to local metal abundance anomalies produced by supernovae and winds from evolved stars, but is also due to measurement errors along with uncertainties associated with the estimation of the distance to the objects. The high sensitivity of SIGGMA will help to improve the estimation of the electron temperature gradient from the data toward H II regions.

We will also be able to measure RRLs from heavier elements such as carbon. Maps of carbon RRL emission in a variety of sources can be used to study PDRs and to test PDR models. SIGGMA can make a great contribution to the study of PDRs because the Arecibo telescope has the sensitivity to map carbon RRLs in a substantial number of sources having a wide range of metallicities.

SIGGMA can help to improve our understanding of the origin and ionization of the ELDM since, owing to its high spatial resolution and high sensitivity, it will map the ELDM up to latitudes of $\sim$2°, thus allowing us to associate the ELDM with individual H II regions.

In summary, we expect the data products and results from SIGGMA to be comparable to those obtained from other surveys such as the Two Micron All Sky Survey (Skrutskie et al. 2006), the *Infrared Space Observatory* (Kessler et al. 1996), the *Midcourse Space Experiment* (Egan et al. 2003), the NVSS (Condon et al. 1998), the Galactic Legacy Infrared Mid-Plane Survey Extraordinaire (Benjamin et al. 2003; Churchwell et al. 2009), and the International Galactic Plane Survey,[11] as well as the G-ALFA Continuum Transit Survey (GALFACTS; Taylor & Salter 2010) and the ALFA Galactic HI Surveys.

2. OBSERVATIONS

2.1. The Receiver

SIGGMA uses the Arecibo *L*-band Feed Array (ALFA)[12] receiver on the Arecibo telescope. The ALFA receiver has seven independent beams, each recording two orthogonal linear polarizations. The beams are arranged in a hexagonal pattern such that there is one central beam (Beam 0) surrounded by six outer beams (Beams 1–6). Due to the optics of the telescope, the outer beams are projected onto an ellipse in the sky. This ellipse is centered on Beam 0 and has semi-axes of 6.′4 in zenith angle by 5.′5 in azimuth. The orientation of the long axis of the ellipse changes with the parallactic angle. Although the array is derotated during observations, the positions of the outer beams change on the sky due to the elliptical projection. This change of outer beams with respect to Beam 0 is typically less than the FWHM of the beam width.

The average FWHM of the beams varies between 3.′3 and 3.′4 across our frequency range.[13] The footprint of all the beams on the sky, out to the ellipse enclosing the FWHM of the outer beams, is (15.′3–18.′6) × (13.′6–16.′5), covering an area of 163–241 arcmin^2. The area falling within the FWHM of the beams is 53–78 arcmin^2, or around a third of the total footprint. The gain of Beams 1–6 is $\sim$8.5 K Jy^{-1}, while Beam 0 has a gain of $\sim$11 K Jy^{-1}. All seven beams have measured system temperatures of 27–28 K at the low zenith angles ($\lesssim$15°)

[11] http://www.ras.ucalgary.ca/IGPS/

[12] See http://www.naic.edu/alfa for more information.

[13] The source of the average FWHM values, as well as the other parameters given in this paragraph, is the Arecibo Observatory's performance and calibration measures, which are made at 1420 MHz. The errors on the beam area introduced by using the average FWHM and a circular beam rather than the true elliptical beam are around one part per thousand, and thus negligible compared to other sources of uncertainty and to the change in beam size over our frequency range.

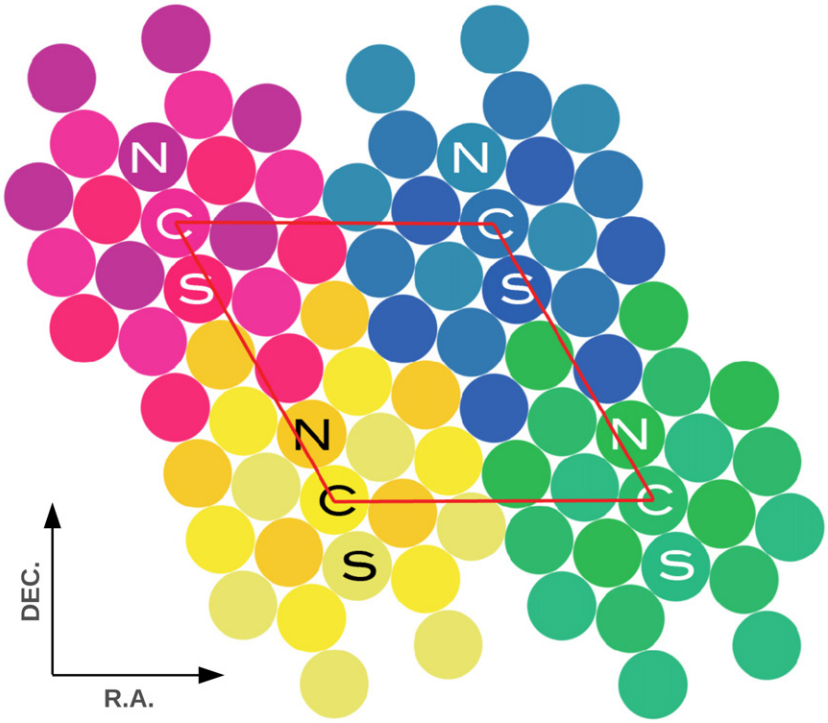

Figure 1. Grid of points used for the RRL survey, with R.A. horizontal and Decl. vertical. Circles indicate the size (FWHM) of the ALFA beams. Circles with the same fill color are observed in the same ALFA pointing; circles with similar fill colors are part of the same pointing cluster, with N, C, and S indicating the north, central, and south pointing of the cluster. The red rhomboid indicates the repeating pattern of the pointing clusters, illustrating that they repeat along lines of constant declination. This figure was developed from Figure 5 of Freire (2003).

(A color version of this figure is available in the online journal.)

where most of our observations will occur, producing a system equivalent flux density of ∼2.5 Jy for Beam 0 and ∼3.2 Jy for Beams 1–6. The receiver has a bandwidth of 300 MHz, covering 1225–1525 MHz.

2.2. The Backend

Spectra are recorded once per second using the Mock Spectrometer, a Fourier-transform device that has two groups, each of 14 boards. This setup enables the Mock Spectrometer to process data from the seven ALFA beams, each of which is divided into two intermediate frequency (IF) sub-bands. The first group is used in a high time-resolution, low spectral-resolution mode to obtain data for the commensal "P-ALFA" pulsar survey (Cordes et al. 2006), while the second group is used to acquire data simultaneously for the RRL survey. Each IF sub-band covers 172 MHz, with the first IF centered at 1450 MHz and the second IF centered at 1300 MHz. Together, these sub-bands cover the entire 300 MHz ALFA bandpass, with the filter roll-off being either in the overlap region between the two sub-bands or outside the band of the receiver.

For the RRL survey, data were accumulated for 1 s before being Fourier transformed to form spectra with 8192 channels per IF sub-band. This procedure gives a spectral resolution of 21 kHz, equivalent to 4.2–5.1 km s^{-1} for the H$n\alpha$ recombination lines within the ALFA bandpass. The required integration time is then built up from multiple 1 s spectra.

2.3. Observing Technique

The survey uses a "leapfrog"-style observing technique (Spitzak & Schneider 1998) with a grid of points that repeat along lines of constant declination (see Figure 1). Each observation integrates on each position for 270 s (180 s in the outer Galaxy). Combined with the slew time, this procedure gives a spacing of nearly five minutes between observations. By choosing pointings from the grid with the same declinations and separated by five minutes in right ascension, we track the same azimuth and zenith angle in consecutive points. This technique allows consecutive points to be used as ON–OFF pairs in order to form a bandpass-corrected (ON–OFF)/OFF spectrum (see Section 3). The five minute separation in time between ON and OFF points provides the best baselines because ripples caused by internal reflections in the antenna, ground pick up, and atmospheric effects mostly cancel out in the corrected spectrum.

The survey tiling pattern is made up of clusters of three pointings that are offset from each other by one beam FWHM beamwidth, labeled as the north (N), central (C), and south (S) pointings in Figure 1. This pattern is a modification of the original P-ALFA pulsar survey tiling pattern (Cordes et al. 2006), with the axis of the pattern (and of the ALFA receiver) rotated by 19 deg from celestial north so that adjacent clusters of pointings fall on lines of constant declination. By leapfrogging through this tiling pattern, the survey covers approximately 10 deg^2 of sky in 100 hr of telescope time. In the outer Galaxy, where SIGGMA is commensal with the ALFA Zone of Avoidance survey, integration times per pointing are shorter but the pattern is observed three times with a small offset (∼1.′9) in order to produce a Nyquist-sampled map of 10 deg^2 of sky to a similar depth in 200 hr of telescope time.

3. DATA REDUCTION

The entire 300 MHz bandpass of the RRL survey observations is divided into two IF sub-bands. Examples of spectra from the two sub-bands are shown in Figures 2 and 3. The two

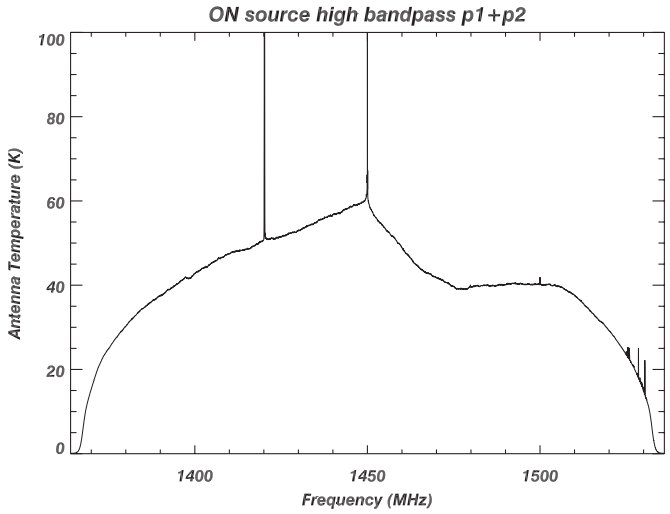

Figure 2. Spectral shape of the raw data for the higher IF sub-band when the antenna beam is on the source S255. This spectrum is produced by averaging over a 270 s exposure. The orthogonal polarizations have also been averaged. The antenna temperature includes about 12 K continuum flux from the source and the spikes are due to RFI.

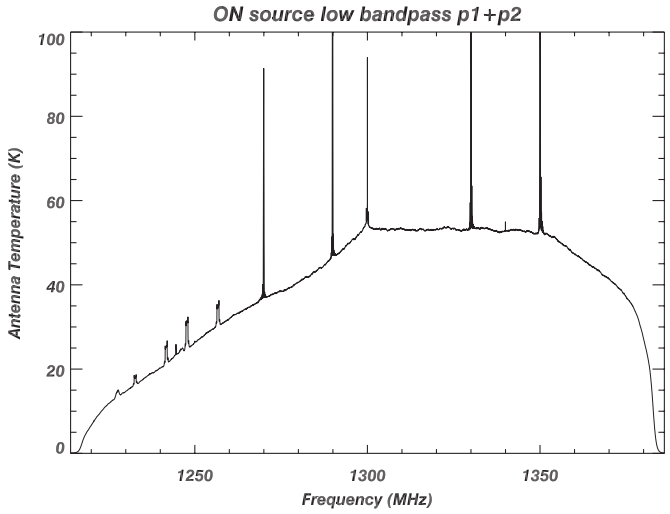

Figure 3. Same as Figure 2 but for the lower IF sub-band.

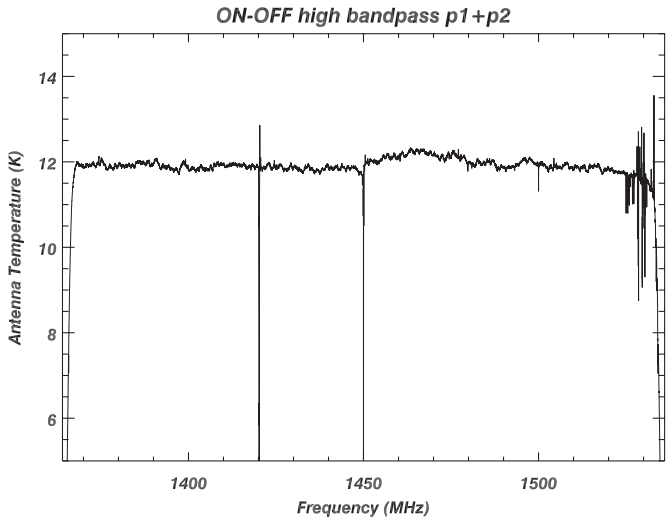

Figure 4. Spectrum after (ON−OFF)/OFF bandpass correction: the higher IF band. The antenna temperature includes about 12 K continuum flux from the source and the spikes are due to RFI.

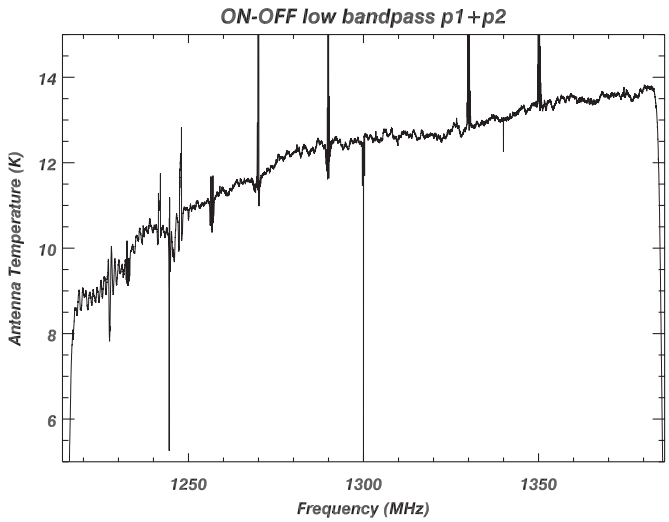

Figure 5. Same as Figure 4 but for the lower IF sub-band.

orthogonal polarizations are averaged for each sub-bandpass, thereby achieving a ∼40% increase in S/N but rendering the data insensitive to polarization.

After matching the ON/OFF pointing pairs, we perform a bandpass correction to the raw ON/OFF spectral pairs via the customary position switched method of (ON–OFF)/OFF × Tsys, where Tsys is the system temperature. Bandpass corrected spectra are shown in Figures 4 and 5. It is clear that the radio frequency interference (RFI) in the higher frequency IF sub-band is considerably less serious than in the case of the lower IF band.

We separate each 300 MHz spectrum into 12 segments, each of which covers ±300 km s^{-1} centered between the rest frequencies of the Hnα and Henα lines such that the Hnα and Henα lines are offset by +61 km s^{-1} and −61 km s^{-1}, respectively, from the band center and the Cnα line is offset −88 km s^{-1} from the band center. The velocity range, with respect to the local standard of rest (LSR), spans the entire velocity of Galactic gas toward each pointing. Table 1 lists the 12 H, He, and C α-transitions located within the full 300 MHz band.

Table 1
The Frequencies of the 12 α-RRL Transitions within the 300 MHz Bandpass

Num	n	Hnα	Henα	Cnα	Central Freq
1	163	1504.608	1505.221	1505.359	1504.9145
2	164	1477.335	1477.937	1478.072	1477.6360
3	165	1450.716	1451.307	1451.440	1451.0115
4	166	1424.734	1425.314	1425.444	1425.0240
5	167	1399.368	1399.938	1400.066	1399.6530
6	168	1374.600	1375.161	1375.286	1374.8805
7	169	1350.414	1350.964	1351.088	1350.6890
8	170	1326.792	1327.333	1327.454	1327.0625
9	171	1303.718	1304.249	1304.368	1303.9835
10	172	1281.175	1281.697	1281.815	1281.4360
11	173	1259.150	1259.663	1259.778	1259.4065
12	174	1237.626	1238.130	1238.243	1237.8780

Notes. Column 1 lists the number of the 12 spectral segments. Column 2 gives the 12 lower quantum numbers. Columns 3–5 are the frequencies of the 12 α lines of H, He, and C in MHz. Column 6 gives the adopted central frequencies of each narrowband spectrum.

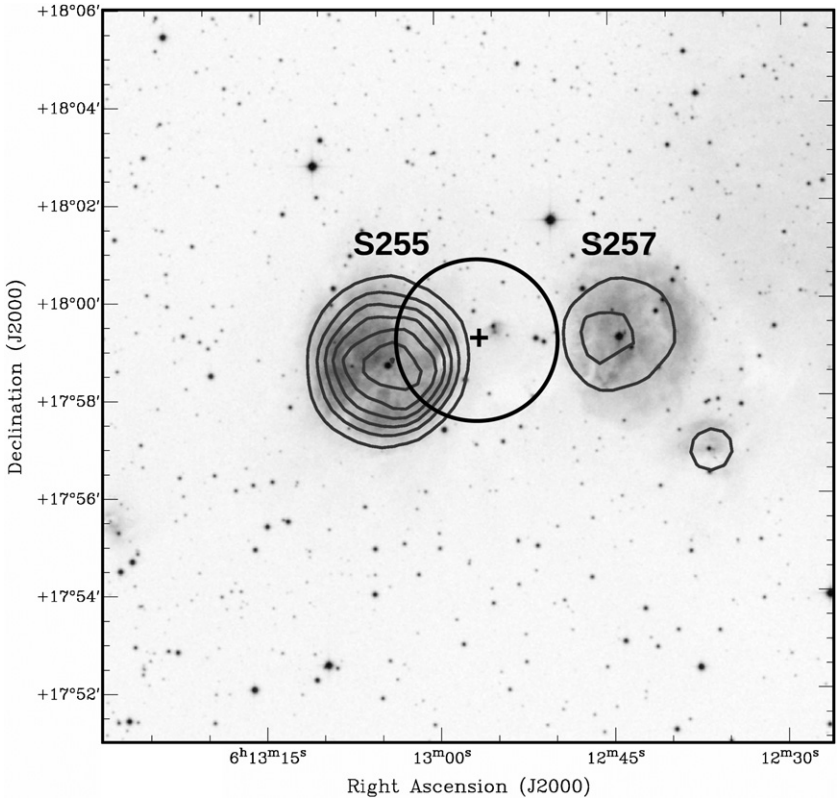

Figure 6. Map of the S255–S257 region, produced by overlapping the NVSS contours on the optical image from the Digitized Sky Survey (DSS; The Digitized Sky Surveys were produced at the Space Telescope Science Institute under U.S. Government grant NAG W-2166. The images of these surveys are based on photographic data obtained using the Oschin Schmidt Telescope on Palomar Mountain and the UK Schmidt Telescope. The plates were processed into the present compressed digital form with the permission of these institutions. See http://stdatu.stsci.edu/dss/index.html.), which has a 1.″7 pixel^{-1} resolution. The plus symbol indicates the beam center of our observations and the open circle shows the 3.′4 beam size.

A 3rd degree polynomial baseline was fit to each of the 12 spectral line segments. The 7th and 12th segments were automatically excised because of bad RFI at these frequencies. Other segments containing channels with strong RFI are flagged and removed manually.

4. A TEST OBSERVATION TOWARD S255

A test observation for SIGGMA was performed toward the H II region S255–S257. The position ($06^h10^m01\overset{s}{.}4$, $+17^d59^m31^s$, B1950) or ($06^h12^m56\overset{s}{.}8$, $+17^d58^m40\overset{s}{.}8$, J2000) was observed with Beam 0. We chose this position because RRLs near 10 GHz were observed earlier by Lockman (1989). However, this position is not the center of the optical or radio nebula, but is offset by ∼1.′5 west of S255 and ∼3′ east of S257 (see Figure 6). In this paper, we refer to this position as S255-west or S255w.

The 12 lines observed toward S255w are shown in Figure 7, where the top six spectra are from the higher sub-band and the bottom six spectra are from the lower sub-band. The Hnα lines can be clearly identified in all the narrowband spectra that are not affected by RFI. Most of the spectra also show recognizable Cnα lines. However, strong RFI completely impacted the H169α and H174α spectra (the 7th and the 12th segments in Figure 7), rendering them unusable. The remaining 10 spectra were re-sampled to the same velocity resolution and averaged to obtain the final spectrum. A fifth-order baseline was fit and subtracted from the final spectrum. Lower order polynomials were tested but they were not sufficient to remove the residual baseline ripple. The final averaged spectrum for S255w has an rms noise level ∼0.5 mJy and is shown in Figure 8. A Gaussian fit to the Hnα feature gives a central LSR velocity of +7.1 ± 0.5 km s^{-1}, with an FWHM of 23.5 ± 0.5 km s^{-1}. The RRL emission at this position detected by Lockman (1989) at 10 GHz has an LSR velocity of +7.5 ± 0.6 km s^{-1} with an FWHM 20.1 ± 1.5 km s^{-1}, which agrees with our detection. The parameters obtained for all the line features in the spectrum are listed in Table 2.

Table 2
The Line Parameters of S255w

	S_L (mJy)	$v_{\rm LSR}$ (km s^{-1})	Δv (km s^{-1})
Hα	15.5 ± 0.6	+7.1 ± 0.5	23.5 ± 0.5
Cα	6.6 ± 0.7	+6.4 ± 0.4	7.2 ± 0.5

Notes. Column 2 is the peak line flux density. Column 3 gives the line velocity. Column 4 shows the line width (FWHM). All the parameters are results of Gaussian fits to the spectrum. The line widths were corrected for the channel width.

The carbon line detected is almost certainly coming from PDRs. Since the temperature of these regions is at least a factor of 10 lower than that of H II regions and carbon is ionized in the PDR, intense carbon RRLs are expected. Carbon RRLs will also be amplified by the background from the H II region (if the PDR is in front of the H II region) and the Galactic background. In order to study the physical properties of these regions, observations of carbon RRLs at several frequencies are needed to compare with models that must take into account the geometry of the region. There is no detection of He RRLs in the spectrum of Figure 8. This result is in agreement with the findings of Silvergate & Terzian (1979), who did not observe He emission in their sensitive RRL spectrum of S255 at 1.4 GHz.

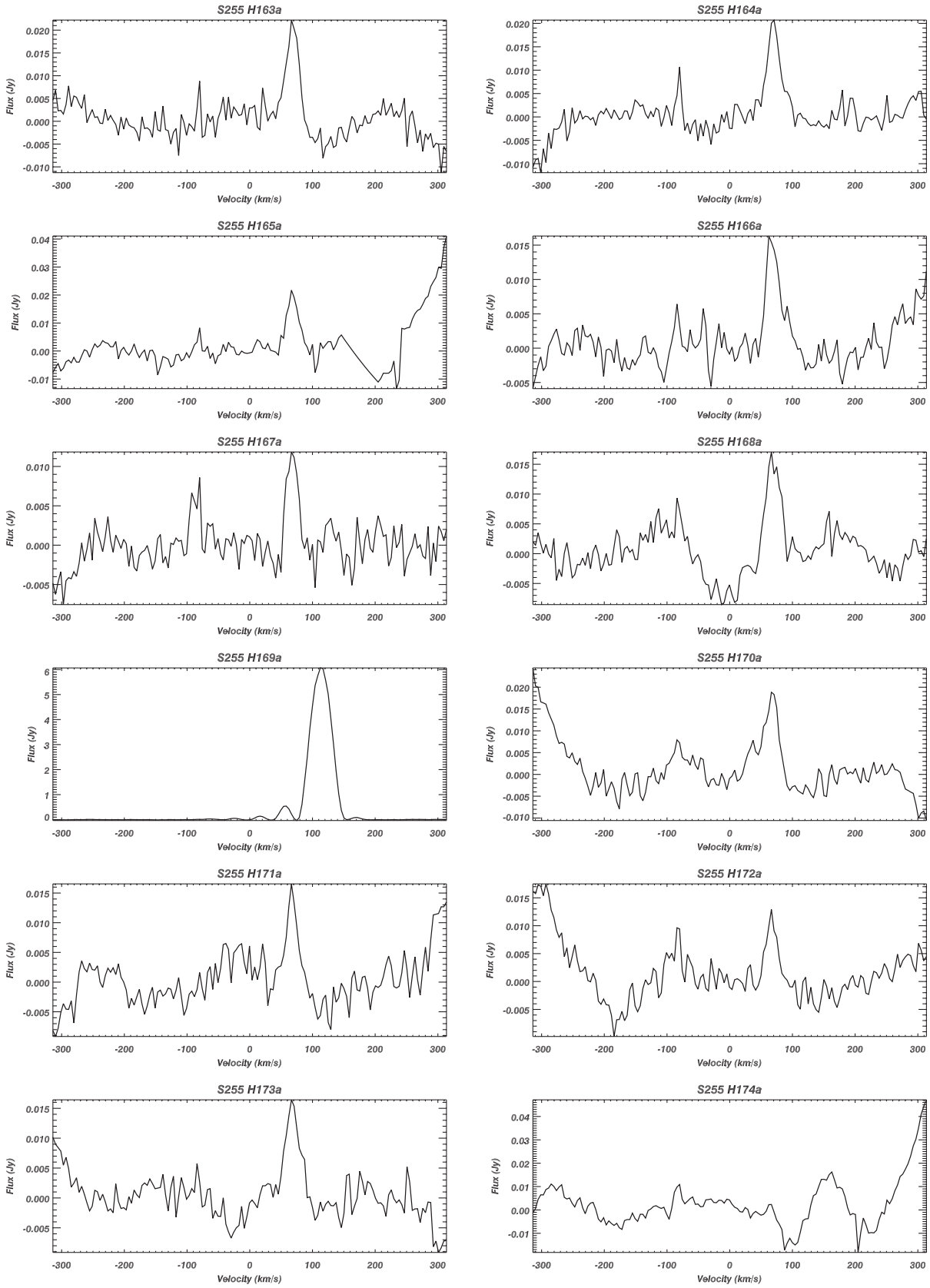

Figure 7. Twelve Hnα lines in the direction of the H II region S255. The H169α and H174α spectra are impacted by RFI. Note that due to the velocity frame set in Section 3, the Hnα, Henα, and Cnα lines lie at +61, −61, and −88 km s^{-1}, respectively, from the origin.

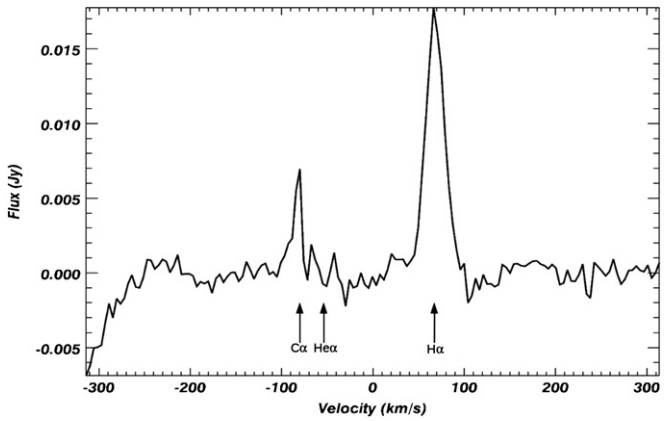

Figure 8. Stacked RRL spectrum for the H II region S255. Note that due to the velocity frame set in Section 3, the Hnα, Henα, and Cnα lines lie at +61, −61, and −88 km s^{-1}, respectively, from the origin. The drop-off on the left-hand edge of spectrum, from −300 to −250 km s^{-1}, is caused by the polynomial baseline fitting and this region has not been included in the calculation of the rms noise of the spectrum.

For a typical He/H RRL ratio of 0.1 (Churchwell et al. 1974), the expected He line strength would be about a 3σ detection. Therefore, the non-detection may be due to the fact that we are not exactly on the source, as the non-detection can also indicate a lower He/H for this region.

5. SUMMARY

SIGGMA will be the most sensitive fully-sampled RRL survey of the Galactic plane observable with the Arecibo Telescope. When complete, this survey will cover 300 deg^2: $30^\circ \leqslant l \leqslant 75^\circ$ and $-2^\circ \leqslant b \leqslant 2^\circ$ in the inner Galaxy; $175^\circ \leqslant l \leqslant 207^\circ$ and $-2^\circ \leqslant b \leqslant 1^\circ$ in the outer Galaxy. SIGGMA provides fully sampled RRL maps with 3.′4 resolution and a line flux density sensitivity ∼0.5 mJy. The observations started in 2010 and have covered an area of ∼50 deg^2 to date. A software pipeline has been developed to process and archive SIGGMA data. The fully sampled data will also be produced as a set of three-dimensional data cubes, each of size 2×4 deg^2 × 151 spectral channels, using the software package Gridzilla (Barnes et al. 2001).

Our test observations toward the S255/S257 H II complex demonstrate the data quality. Hydrogen and carbon lines were detected with good S/N. To derive reliable physical parameters such as the electron temperature and density, as well as metal abundances from SIGGMA data, total continuum data are needed. These will be provided by GALFACTS (Taylor & Salter 2010), whose observations will be completed in 2013. We expect to finish observations of regions covering W49 and W51 in the next few months. These observations will be analyzed using the data reduction pipeline developed and will provide early science results for the survey.

We thank the anonymous referee for useful comments on this manuscript. We are grateful to C. Salter for helpful discussions and comments. We acknowledge the Arecibo Observatory. The Arecibo Observatory is operated by SRI International under a cooperative agreement with the National Science Foundation (AST-1100968) in alliance with Ana G. Méndez-Universidad Metropolitana and the Universities Space Research Association. B.L. acknowledges the hospitality enjoyed as a visiting student at the Arecibo Observatory and Cornell University. B.L. is partly supported by the China Ministry of Science and Technology under the State Key Development Program for Basic Research (2012CB821800, 2013CB837900) and the Projects of International Cooperation and Exchanges NSFC (11261140641).

REFERENCES

Afflerbach, A., Churchwell, E., Acord, J., et al. 1996, ApJS, 106, 423
Afflerbach, A., Churchwell, E., & Werner, M. W. 1997, ApJ, 478, 190
Alves, M. I. R., Davies, R. D., Dickinson, C., et al. 2010, MNRAS, 1669, 1654
Alves, M. I. R., Davies, R. D., Dickinson, C., et al. 2012, MNRAS, 422, 2429
Anantharamaiah, K. R. 1986, JApA, 7, 131
Anderson, L. D., Bania, T. M., Balser, D. S., & Rood, R. T. 2011, ApJS, 194, 32
Baddi, R. 2012, AJ, 143, 26
Bania, T. M., Anderson, L. D., Balser, D. S., & Rood, R. T. 2010, ApJL, 718, L106
Barnes, D. G., Staveley-Smith, L., de Blok, W. J. G., et al. 2001, MNRAS, 322, 486
Benjamin, R. A., Churchwell, E., Babler, B. L., et al. 2003, PASP, 115, 953
Churchwell, E., Babler, B. L., Meade, M. R., et al. 2009, PASP, 121, 213
Churchwell, E., Mezger, P. G., & Huchtmeier, W. 1974, A&A, 32, 283
Churchwell, E., & Walmsley, C. M. 1975, A&A, 38, 451
Condon, J. J., Cotton, W. D., Greisen, E. W., et al. 1998, AJ, 115, 1693
Cordes, J. M., Freire, P. C. C., Lorimer, D. R., et al. 2006, ApJ, 637, 446
Davies, R. D., Matthews, H. E., & Pedlar, A. 1972, NPhS, 238, 101
Dravskikh, Z. V., Dravskikh, A. F., & Kolbasov, V. A. 1966, IAU Trans., XIIB, 360
Egan, M. P., Price, S. D., & Kraemer, K. E. 2003, BAAS, 35, 1301
Freire, P. C. C. 2003, Optimal Tiling for Non-Drifting ALFA Surveys (ALFA Tech. Memo Series; Arecibo: Arecibo Observatory), http://www.naic.edu/alfa/memos/
Gordon, M. A., & Sorochenko, R. L. 2002, Radio Recombination Lines: Their Physics and Astronomical Applications (1st ed; Berlin: Springer)
Gottesman, S. T., & Gordon, M. A. 1970, ApJL, 162, L93
Hart, L., & Pedlar, A. 1976, MNRAS, 176, 547
Heiles, C. 1994, ApJ, 436, 720
Heiles, C., Reach, W. T., & Koo, B.-C. 1996, ApJ, 466, 191
Höglund, B., & Mezger, P. G. 1965, Sci, 150, 339
Kessler, M. F., Steinz, J. A., Anderegg, M. E., et al. 1996, A&A, 315, L27
Lee, E. J., Murray, N., & Rahman, M. 2012, ApJ, 752, 146
Lockman, F. J. 1976, ApJL, 209, 429L
Lockman, F. J. 1989, ApJS, 71, 469
Mezger, P. G. 1978, A&A, 70, 565
Palmer, P., Zuckerman, B., Penfield, H., Lilley, A. E., & Mezger, P. G. 1967, Natur, 215, 40
Pankonin, V., Walmsley, C. M., Wilson, T. L., & Thomasson, P. 1977, A&A, 57, 341
Peek, J. E. G., Heiles, C., Douglas, K. A., et al. 2011, ApJS, 194, 208
Petuchowski, S. J., & Bennett, C. L. 1993, ApJ, 405, 591
Reifenstein, E. C., Wilson, T. L., Burke, B. F., Mezger, P. G., & Altenhoff, W. J. 1970, A&A, 4, 357
Reynolds, R. J. 1990, ApJL, 349, L17
Roshi, D. A., & Anantharamaiah, K. R. 2000, ApJ, 535, 231
Roshi, D. A., & Anantharamaiah, K. R. 2001, ApJ, 557, 226
Roshi, D. A., & Kantharia, N. G. 2011, MNRAS, 414, 519
Roshi, D. A., Plunkett, A., Rosero, V., & Vaddi, S. 2012, ApJ, 749, 49
Shaver, P. A. 1976, A&A, 49, 1
Shaver, P. A., McGee, R. X., Newton, L. M., Danks, A. C., & Pottasch, S. R. 1983, MNRAS, 204, 53
Silvergate, P. R., & Terzian, Y. 1979, ApJS, 39, 157
Skrutskie, M. F., Cutri, R. M., Stiening, R., et al. 2006, AJ, 131, 1163
Sorochenko, R. L., & Borodzich, E. V. 1966, IAU Trans., XIIB, 360
Spitzak, J. G., & Schneider, S. E. 1998, ApJS, 119, 159
Taylor, A. R., & Salter, C. J. 2010, in ASP Conf. Ser. 438, The Dynamic Interstellar Medium: A Celebration of the Canadian Galactic Plane Survey, ed. R. Kothes, T. L. Landecker, & A. G. Willis (San Francisco, CA: ASP), 402
Taylor, J. H., & Manchester, R. N. 1977, ARA&A, 15, 19
Wenger, T. V., Bania, T. M., Dana, S., & Anderson, L. D. 2013, ApJ, 764, 34
Wilson, T. L. 1980, Radio Recombination Lines, Vol. 80 (Dordrecht: Reidel), 205
Wilson, T. L., Mezger, P. G., Gardner, F. F., & Milne, D. K. 1970, A&A, 6, 364